A MULTI-LAYER SILICON MICROSTRIP DETECTOR FOR SINGLE PHOTON COUNTING DIGITAL MAMMOGRAPHY

F. Arfelli[1], V. Bonvicini[1], A. Bravin[1], G. Cantatore[1], E. Castelli[1], L. Dalla Palma[2], M. Fabrizioli[3], R. Longo[1], A. Olivo[1]*, S. Pani[1], D. Pontoni[3], P. Poropat[1], M. Prest[1], A. Rashevsky[1], L. Rigon[3], G. Tromba[3], A.Vacchi[1] and E. Vallazza[1].
[1] Dipartimento di Fisica - Università di Trieste and INFN - Sezione di Trieste
[2] Istituto di Radiologia - Università di Trieste
[3] Sincrotrone Trieste SCpA
* Corresponding Author (olivo@trieste.infn.it)

PAPER PRESENTED AT
MIDEM´98 CONFERENCE – Minisymposium on Semiconductor Radiation Detectors
23.09.98 – 25.09.98, Rogaška Slatina, Slovenia

Keywords: Si silicon microstrip detectors, single photon counting, synchrotron radiation, digital mammography, contrast resolution, spatial resolution, detection efficiency, counting rate, Si silicon microstrip detectors, FOXFET, Field OXide Field Effect Transistors, two-dimensional images, synchrotron radiation, imaging devices, digital imaging devices, CT, computer tomography, MTF, Modulation Transfer Functions

Abstract: The SYRMEP / FRONTRAD (SYnchrotron Radiation for MEdical Physics / FRONTier RADiology) collaboration has developed a digital X-Ray imager for the mammography beamline at ELETTRA, the synchrotron radiation facility in operation in Trieste, Italy. This imaging device is composed of three stacked layers of FOXFET-biased silicon microstrip detectors, positioned with the strips along the beam direction. In this way a very high absorption efficiency is guaranteed, since the strip length (1 cm) absorbs nearly all the incoming photons in the energy range of interest (15 - 30 keV). Furthermore, the active surface is by construction subdivided into pixels, the dimensions of which are determined by the strip pitch (200 μm) in one direction and by the thickness of the single layer (300 μm) in the other. Each layer has 256 implanted strips, and therefore the whole device has an active surface of ~50x1 mm^2 subdivided into 764 pixels (the inter-layer distance is nearly equal to 100 μm).
The electronic chain reading out the detector signal operates in "single photon counting" mode: this gives the possibility of extracting the maximum information from the radiation beam, since the only limitation to the signal-to-noise ratio in the images is the quantum noise.
Two-dimensional images are obtained by scanning the samples through the synchrotron laminar beam, while the detector is kept stationary with respect to the beam itself. The desired statistics is obtained by combining the information from the three layers, thus reducing the overall acquisition time by a factor of three.
Results from extensive tests carried out on this imaging device by means of a synchrotron radiation beam are reported on this paper.

Večplastni silicijev mikropasovni detektor za digitalno mamografijo s štetjem posameznih fotonov

Ključne besede: Si detektorji silicijevi mikrotrakasti, štetje fotonov posameznih, sevanje sinhrotronsko, mamografija digitalna, ločljivost kontrastna, ločljivost prostorska, učinkovitost detekcije, hitrost štetja, Si detektorji silicijevi mikrotrakasti, FOXFET transistorji z učinkom polja, poljsko-oksidni, slike dvodimenzionalne, sevanje sinhrotronsko, naprave upodabljalne, naprave upodabljalne digitalne, CT tomografija računalniška, MTF funkcije prenosne modulacijske

Izvleček: V okviru projekta SYRMEP/FRONTRAD je bila razvit sistem za digitalno slikanje z rentgenskimi žarki za mamografsko žarkovno linijo ELETTRA, sinhrotronskem izvoru pri Trstu v Italiji. Sistem sestavljajo tri plasti mikropasovnih detektorjev, napajanih preko FOXFET struktur, postavljenih s pasovi v smeri žarka. Na ta način zagotovimo visoko stopnjo absorpcije, saj dolžina pasu (1 cm) zagotavlja absorpcijo skoraj vseh vpadnih fotonov v energijskem območju, ki nas zanima (15 – 30 keV). Nadalje, aktivna površina je razdeljena na slikovne elemente, katerih dimenzija je določena s širino in razdaljo med pasovi (200 μm) v eni smeri in z debelino ene plasti (300 μm) v drugi smeri. Vsaka plast vsebuje 256 implantiranih pasov tako, da ima celoten element aktivno površino okoli 50x1 mm^2 razdeljeno na 764 slikovnih elementov (razdalja med notranjimi plastmi je okoli 100 μm).
Elektronika, ki odčitava signale iz detektorja, šteje posamezne fotone, kar predstavlja maksimalno informacijo o prepuščenih žarkih, saj omejujejo signal šum na sliki le statistične fluktuacije.
Dvodimenzijske slike dobimo s premikanjem vzorca znotraj laminarnega sinhrotronskega žarka, med tem ko detektor miruje glede na curek. Željeno statistiko dobimo z upoštevanjem informacije iz treh plasti, s čimer skrajšamo čas meritve za trikrat.V pričujočem prispevku podajamo rezultate testov, ki smo jih opravili z opisanim sistemom v sinhrotronski žarkovni liniji.

INTRODUCTION

Since the introduction of computed tomography by Housenfield (1973), digital radiology has been acquiring more and more relevance /1/. The wide dynamic range of digital imaging devices brings great advantages with respect to the low dynamic range of conventional film-screen systems: it allows one to eliminate exposure constraints and to amplify the contrast of all the regions of interest in the image by means of computer processing. Furthermore, all storage and archival procedures of radiological images would be dramatically simplified if digital data (instead of analogical films) were handled.

Recently, research has also been carried out on the "source side", demonstrating that a laminar monochromatic synchrotron radiation beam allows great improvements in image quality, together with a reduction in the dose delivered to the sample (see for example /2/). The SYRMEP/FRONTRAD collaboration is carrying out a project that aims at improving the quality of mammographic examinations by operating both on the source and on the detector side. A synchrotron radiation monochromatic X-ray beam is used as the illuminating source, and a silicon pixel detector is utilized to collect the photons transmitted through the sample.

The monochromaticity of the radiation beam gives us the possibility of selecting the appropriate energy for each imaging requirement, thus maximizing the image contrast while minimizing the dose delivered to the sample. The intrinsic high collimation of synchrotron laminar beams highly suppresses the defocusing effect that occurs when the source size is large, as in conventional radiology where X-ray tubes are used. Finally, since the laminar beam cross section can be matched (by means of a slit system) with the detector active surface, the detection of scattered radiation is highly reduced.

Silicon microstrip detectors used in a "edge-on" geometrical configuration, i.e. with radiation impinging on the side rather than on the surface of the chip, allow a very high absorption efficiency (~80% @ 20 keV): since the delivered dose is inversely proportional to the detection efficiency, this last parameter is of primary importance for dose minimization purposes. Furthermore, the single photon counting capability of the readout electronics maximizes the device contrast resolution, the only limitation being the quantum noise.

Several detector prototypes have been tested and utilized to produce digital images of mammographic phantoms and of *in vitro* breast tissue specimens /3-6/. The present prototype has been obtained by stacking three silicon layers one upon the other, in order to form a wider sensitive area covering a large part of the beam cross-section and, above all, in order to reduce by a factor of three the overall duration of the examination. The results of the tests carried out on this prototype are discussed in the present article.

MATERIALS AND METHODS

The tests described in this paper have been carried out at the SYRMEP beamline /7/ at the ELETTRA storage ring in Trieste, Italy. The source is one of the 24 bending magnets of the ring. The white beam, with a spectrum ranging from 0 to ~35 keV, is first filtered by a water cooled beryllium window, which takes away the low energy components. Then a channel-cut, Si(1,1,1) crystal is used to filter the spectrum by means of Bragg reflection. This monochromator device provides a monochromatic, tuneable energy beam in the energy range 8-35 keV with an energy resolution of about 0.2%. A tungsten slit system is placed in the vacuum tube immediately before the monochromator, in order to reduce the cross section of the beam impinging on the crystal. At the entrance of the experimental hutch a second tungsten slit system, moved by 1 μm resolution stepping motors, determines the cross section of the beam reaching the detector active surface, which is kept stationary with respect to the beam itself. An ionization chamber, read out by a Keithley amperometer, is placed immediately after the slit system to monitor the photon flux in order to evaluate the dose delivered to the samples. In order to obtain the twodimensional images a micropositioning stage (1 μm resolution), placed between ionization chamber and detector, scans the samples through the beam. A dedicated C/C++ software developed on a LINUX operating system running on a Pentium PC controls both the sample movement and the readout system. The core of the front-end electronics consists in a series of 32-channel mixed analog-digital VLSI chips (CASTOR /8/) housed on 7-layer ceramic hybrid circuits. Each VLSI channel features a charge sensitive preamplifier, a CRRC shaper, a high-pass filter, a threshold discriminator and a 16 bit counter which counts the signals from single photons with a rate of ~10^4 counts/s. A modular set of PCB cards allows the prompt expansion of the front-end electronics in order to run imager versions with an increasing number of channels. The same choice has been made for the readout electronics, which is based on a CAMAC board.

The detector prototype discussed in this paper has been obtained by stacking three single microstrip detectors one upon the other. The peculiar trapezoidal shape of these silicon chips allows the connection of each strip to the front-end electronics by means of flexible upilex fan-outs. Two full trapezoidal structures (each one featuring 256 200 μm channels) and two half structures (featuring 128 200 μm channels) have been assembled (see Fig. 1), in order to leave enough space for wire bonding behind the assembled prototype. This device has been used to produce digital images of several test objects, in order to determine its perform-

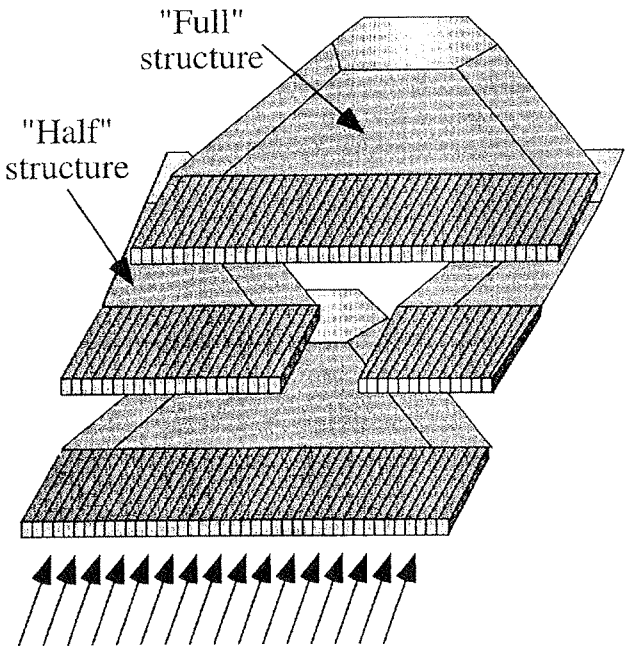

Fig. 1. Schematic layout of the three-layer detector assembly. Two "full" and two "half" trapezoidal structures are used, in order to leave enough space for the wire bonding behind the assembled structure.

ances in terms of contrast and spatial resolution. In particular a "Contrast-Detail Phantom", consisting in a plexiglass slab containing several air disks of different thicknesses and diameters, has been used to measure the contrast resolution, and a bar pattern test object, i.e. a lead mask in which several line patterns of different size and spacing are carved, has been imaged in order to test the spatial resolution.

RESULTS AND DISCUSSION

The detector prototype, aligned with the incoming synchrotron beam, has been tested at the SYRMEP beamline. All the results described below have been obtained with a beam energy equal to 20 keV, and with the slit system set to obtain a beam cross-section equal to 50x1.1 mm^2, matching the detector active surface.

First of all, the detector has been illuminated with different values of the incoming flux, obtained by placing several aluminum filters of different calibrated thicknesses in front of the ionization chamber and of the detector system. The detected rate (counts/pixel/s) has been plotted against the incoming rate, measured using the previously calibrated ionization chamber (a cross-check on these values has been done by taking into account the aluminum absorption coefficient and the thickness of the filters). The result of this preliminary measurement is shown in Fig. 2. The experimental points have been fitted assuming a non paralyzable model for the detector behavior /9/:

$$M = \frac{\varepsilon \cdot R}{1 + \varepsilon \cdot R \cdot \tau} \qquad (1)$$

where M is the detected rate per pixel (counts/pixel/s), R the incident rate per pixel (counts/pixel/s), ε the detection efficiency @20 keV (assuming a very low rate: it is practically the slope of the curve at the origin) and τ the dead time of the prototype. As can be seen from Fig.2, the assumed model fits very well the experimental data (the reduced χ^2 is equal to 0.78). The estimates for dead time and efficiency obtained from the fit are $\tau = 16.7 \pm 0.3$ μsec, $\varepsilon = 80 \pm 2\%$, respectively. The limitation in the detection efficiency stems from the presence of a dead zone in the active volume of the detector:

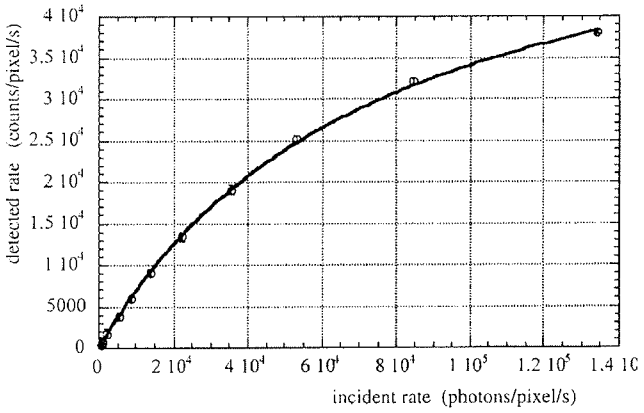

Fig. 2. Detected rate VS. incident rate. The experimental points (dots) have been fitted by means of a non-paralyzable model (solid line, see text for description).

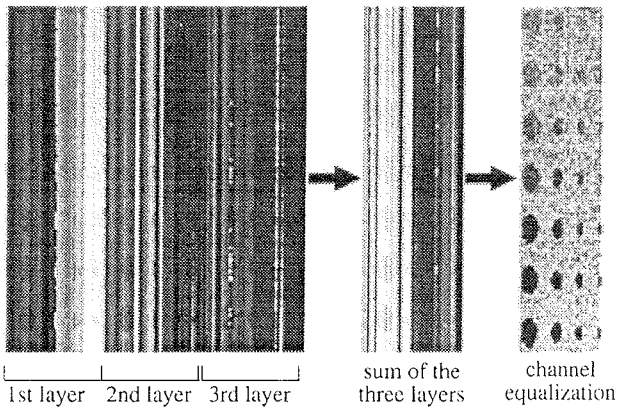

Fig. 3. Image reconstruction procedure. The processed image is obtained by summing the images acquired by each one of the three layers and by equalizing the different gains of each channel (see text).

photons absorbed in the first slice of the detector, where the electric field is veiy low, are not detected. This is due to the necessity of preserving a certain distance between the implanted strips and the physical edge of the chip, in order to avoid a dramatic increase of the reverse dark current. Several tests have been carried out to find the "cut" distance that maximizes the detection efficiency while minimizing the reverse dark current /10/, resulting in a "cut" distance of the present prototype equal to 250 μm, which is fully compatible with an efficiency of 80% at 20 keV. As it can be seen in Fig. 2, the first counting losses occur already at about 10^4 counts/pixel/s: as discussed below, this has a non negligible influence on imaging results.

The image reconstruction process is illustrated in Fig. 3, where three different stages of the procedure are shown for an image of the "Contrast-Detail" phantom. Fig. 3a shows the raw data: the three different images of the phantom, each one acquired by a different layer of the detector, are shown. Fig. 3b shows the sum of these three images: the number of counts per image pixel is increased by a factor of three, reaching the desired statistics of 10^4 photons per pixel. Obviously, in order to obtain the same statistics with a single layer detector, an exposure time increased by a factor three would be necessary. The image still presents some artifacts - due to the gain differences between different channels obscuring the details: in order to correctly visualize the imaging result a channel equalization is necessary. Fig. 3c shows the result of this equalization procedure: the artifacts are eliminated and the details are clearly visible.

As discussed above, images of a Contrast-Detail phantom are used to estimate the contrast resolution of the imaging device. Due to the saturation effect shown in Fig. 2, the incident rate will have a strong influence on the detected contrast. Fig. 4 demonstrates this effect: images of the Contrast-Detail phantom have been acquired at three different values of the incident rate: 5, 16 and 65 kHz, and the corresponding values of the contrast of each disk have been measured for a set of disks

of increasing thicknesses. The contrast is estimated by applying the following definition /11/:

$$\frac{N_1 - N_2}{(N_1 + N_2)/2} \cong \frac{N_1 - N_2}{N_1} \qquad (2)$$

where N_2 are the counts per unit surface occurring in the image in correspondence of the detail and N_1 the counts per unit surface immediately outside it. The introduced approximation works well when low contrasts are examined.

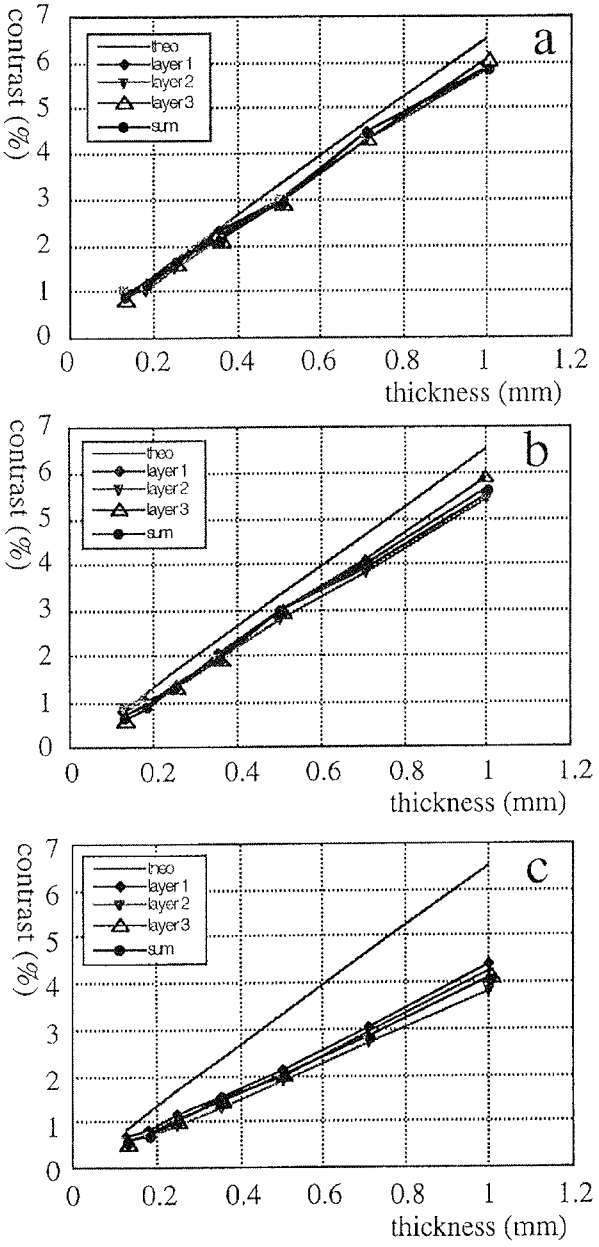

Fig. 4. Detected VS. theoretical contrast as a function of the disk thickness, extracted from the processed image visible in Fig. 3. The same procedure has been applied for three data sets acquired at three different counting rates: 5, 16 and 65 kHz. The loss in the detected contrast grows as the rate is increased (see text).

In Fig. 4a (5 kHz), 4b (16 kHz) and 4c (65 kHz) five point series are represented: the theoretical contrast of the disks, the contrast measured by means of each single detector layer and the contrast estimated from the image obtained by summing the three layers. First of all, one notices that the contrast obtained from the sum of the three layers always lays in the middle of the values obtained from each single layer, meaning that no contrast resolution is lost when the image reconstruction procedure is applied. On the other hand, the contrast resolution losses that occur as the rate is increased are apparent. At present, the maximum counting rate that can be accepted in order to avoid relevant contrast resolution losses is of the order of 10 kHz. It is however important to notice that in all cases contrast values of the order of 1 % are detected, while with conventional screen-film systems contrast values lower than 2-3% are undetectable.

The last part of this discussion deals with spatial resolution measurements. It is important to notice that - even if the pixel size is equal to 200x300 μm^2 - it is possible to obtain images with improved spatial resolution, at least in the direction in which the samples are scanned through the beam. In fact, if a scanning step smaller than the pixel size is chosen, the acquired "raw" image will consist of the convolution between the "real" image and the Point Spread Function of the detector /12/. By applying then simple algorithms performing deconvolution and filtration, it is possible to obtain an image with a spatial resolution determined by the scanning step rather than by the pixel size. Fig. 5 shows an example of this procedure: the same portion of the bar pattern test object discussed above has been imaged both with a sampling step equal to the pixel size (300 μm, Fig. 5a), and with a sampling step much smaller than the pixel size (20 μm, Fig. 5b: the presented image has already been deconvoluted and filtered). All the bar patterns are indicated by their spatial frequency expressed in line pairs per mm: 3 lp/mm indicates for instance lead bars having dimensions equal to ~167 μm. According to the Nyquist theorem /13/, all these details are invisible if the spatial sampling is equal to 300 μm, as demonstrated by Fig. 5a; while with a sampling step equal to 20 μm all the details must be detected, as shown in Fig. 5b.

The bar pattern test object inputs a fixed spatial frequency to the imaging device, allowing an estimate of the Modulation Transfer Function (MTF, /12/) of the device itself. Fig. 6 shows the comparison between the theoretical MTF of a 300 μm pixel (dashed line) and the theoretical MTF of a 20 μm pixel (solid line). The dots represent the experimental points extracted from the measurement made with a sampling step equal to 20 μm, and demonstrate that our procedure approximates very well the spatial resolution that would be provided by a pixel having dimensions equal to the selected sampling step. Values extracted from measurements obtained by each detector layer are presented for each spatial frequency, and they are compared to the values extracted from the sum of the images acquired by each layer. As in the case of the contrast resolution, the fact that values coming from the reconstructed image lay always within values coming from each layer demonstrates that no spatial resolution is lost when the image reconstruction procedure is applied.

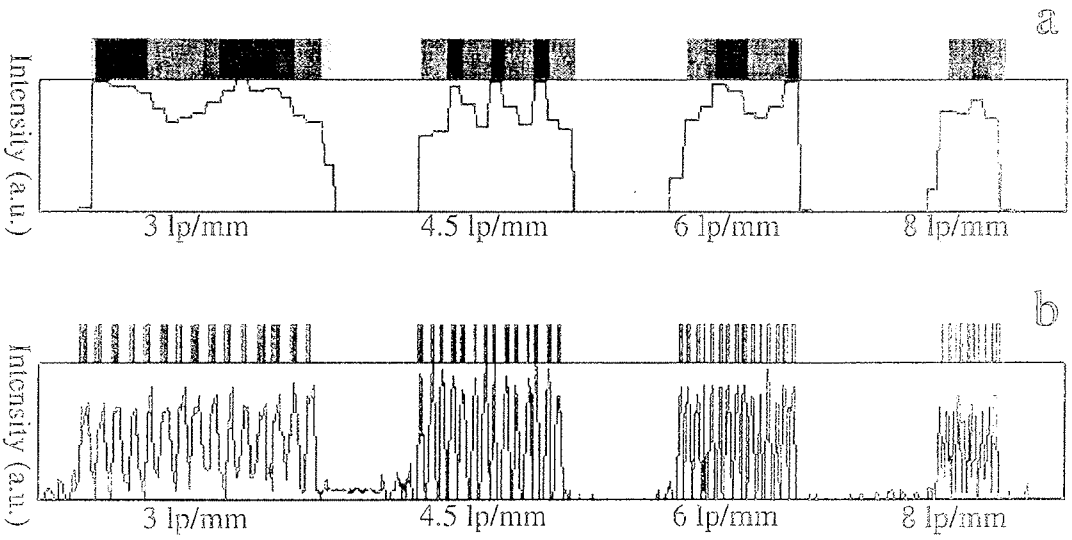

Fig. 5. Images of a bar pattern test object. The first one (a) has been acquired with a sampling step equal to the pixel size (300 μm), while the second one (b) has been acquired with a sampling step much smaller than the pixel size (20 μm), and then deconvoluted and filtered.

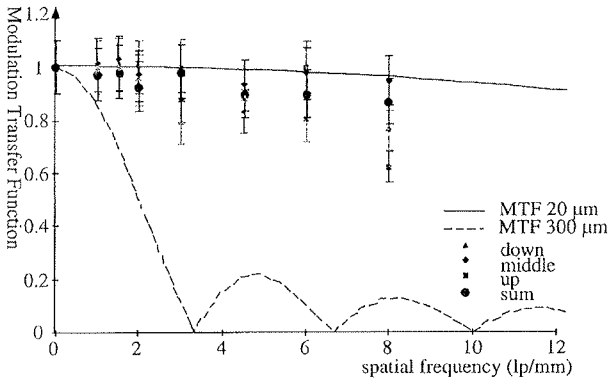

Fig. 6. Modulation Transfer Function of the device when samples are imaged with a scanning step equal to 20 μm, compared to the theoretical MTF of a 300 μm pixel. The plot demonstrates the possibility of achieving enhanced spatial resolution by applying the deconvolution procedure (see text).

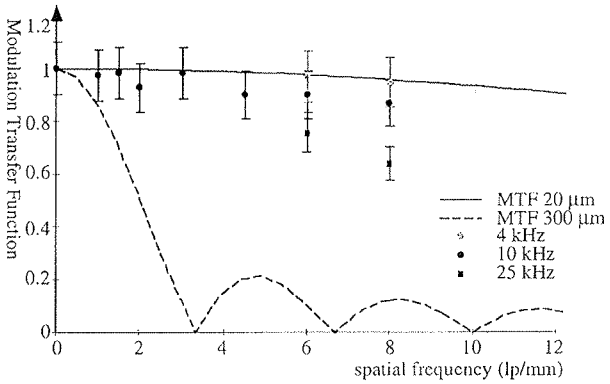

Fig. 7. Modulation Transfer Function of the device (when samples are radiographed with a scanning step equal to 20 μm) as a function of the incident rate. Saturation problems that occur at high rates affect also the spatial resolution of the device (see text).

Finally, the effect of high-rate saturation on spatial resolution has been estimated. The results presented in Fig. 5 and Fig. 6 have been obtained with a counting rate equal to 10 kHz; for comparison purposes the higher spatial frequencies of the bar pattern test object have been also acquired at counting rates equal to 4 and 25 kHz. The results are presented in Fig. 7: only data coming from the sum of the three layers are shown. As it can be easily seen, there is a slight improvement in spatial resolution if the acquisition is performed at 4 kHz, while a non negligible loss occurs if the counting rate is increased to 25 kHz.

CONCLUSIONS

A three layer single photon counting silicon microstrip detector has been developed by the SYRMEP/FRONTRAD collaboration, in order to perform feasibility studies on digital mammography with synchrotron radiation. The device has been extensively tested at the SYRMEP beamline, in order to evaluate its imaging performances. Due to the single photon counting capability of the readout electronics, the contrast resolution is very high, limited in practice only by the quantum noise. The spatial resolution can be very good, since it is possible to increase it by selecting a sampling step smaller than the pixel size. Images are almost scatter free, since the laminar synchrotron beam is matched to the detector active surface by means of a micrometric

slit system. The detection efficiency is high (80% @ 20 keV), and this results in a dose delivered to the samples much lower than doses delivered in conventional mammographic examinations (even if this aspect has not been discussed in the present paper, detailed dose considerations can be found in /3/ and in /6/).

The tested device shows relevant limitations in the counting rate, due to the single photon counting modality chosen for the readout electronics. As discussed in this article, the single photon counting capability is of primary importance in digital mammography, since it maximizes the contrast resolution. In order to solve this problem, two strategies are under investigation. The first one - discussed in the present paper - is the possibility of stacking several detector layers one upon the other: the overall duration of the examination is reduced by a factor equal to the number of stacked layers. Secondly, a faster, second generation single photon counting readout electronics is currently under test: the design features and the simulations predict the possibility of reaching a counting rate at least 30 times higher than the present one.

REFERENCES

/1/ M.J. Yaffe and J.A. Rowlands, *X ray detectors for digital radiography,* Phys. Med. Biol. 42 (1997) 1-39

/2/ E. Burattini, E. Cossu, C. Di Maggio et al., *Mammography with synchrotron radiation,* Radiology 200 (1996) 659-663

/3/ F. Arfelli, V. Bonvicini, A. Bravin et al., *Linear array silicon pixel detector: images of a mammographic test object and evaluation of delivered doses,* Phys. Med. Biol. 42 (1997) 1565-1573

/4/ F. Arfelli, V. Bonvicini, A. Bravin et al., *Design and evaluation of AC-coupled, FOXFET biased, "edge-on" silicon strip detector for X ray imaging,* Nucl. Instrum. Meth. Phys. Res. 385 A (1997) 511-520

/5/ F. Arfelli, V. Bonvicini, A. Bravin et al., An *"edge on" silicon strip detector for X ray imaging,* IEEE Trans. Nucl. Sci. 44 (1997) 874-880

/6/ F. Arfelli, V. Bonvicini, A. Bravin et al., *Mammography of a phantom and breast tissue with synchrotron radiation and a linear-array silicon detector,* Radiology 208 (1998) 709-715

/7/ F. Arfelli, A. Bravin, G. Barbiellini et al., *Digital mammography with synchrotron radiation,* Rev. Sci. Instrum. 66 (1995) 1325-1328

/8/ C. Colledani, G. Comes, W. Dulinsky et al., *CASTOR* I.O, *a VLSI analog-digital circuit for pixel imaging applications,* Nucl. Instrum. Meth. Phys. Res. 395 A (1997) 435- 442

/9/ G.F. Knoll, *Radiation detection and measurements* (II edition), Wiley, New York, 1989

/10/ F. Arfelli, V. Bonvicini, A. Bravin et al., *New developments in the field of silicon detectors for digital radiology,* Nucl. Instrum. Meth. Phys. Res. 377 A (1996) 508-513

/11/ S. Webb ed, *The physics of medical imaging,* IOP publishing, Bristol,1988

/12/ A.L. Evans, *The evaluation of medical images,* Adam Hilger Ltd, Bristol,1981

/13/ E.O. Brigham, *The Fast Fourier Transform,* Prentice Hall, Englewood Cliffs. New Jersey,1974

F. Arfelli, V. Bonvicini, A. Bravin, G. Cantatore,
E. Castelli, A.Vacchi, E. Vallazza, R. Longo,
A. Olivo, S. Pani, P. Poropat, M. Prest, A. Rashevsky
Dipartimento di Fisica -
Università di Trieste and INFN -
Sezione di Trieste

L. Dalla Palma,
Istituto di Radiologia - Università di Trieste

L. Rigon, G. Tromba, M. Fabrizioli, D. Pontoni
Sincrotrone Trieste SCpA

Corresponding Author (olivo@trieste.infn.it)

Prispelo (Arrived) : 29.01.1999 Sprejeto (Accepted) : 03.03.1999